# On the estimation of landslide intensity, hazard and density via data-driven models

Mariano Di Napoli[a,1], Hakan Tanyas[b], Daniela Castro-Camilo[c], Domenico Calcaterra[d], Andrea Cevasco[a], Diego Di Martire[d], Giacomo Pepe[a], Pierluigi Brandolini[a], Luigi Lombardo[b,1,2]

[a]Department of Earth, Environment and Life Sciences, University of Genoa, Corso Europa, 26, 16132 Genoa, Italy; [b]Department of Earth System Analysis, Faculty of Geo-Information Science and Earth Observation (ITC), University of Twente, PO Box 217, Enschede, AE 7500, Netherlands; [c]School of Mathematics and Statistics, University of Glasgow, Glasgow, G12 8QQ, UK; [d]Department of Earth, Environment and Resources Sciences, Federico II University of Naples, Naples 80138, Italy.

Corresponding author: Luigi Lombardo.

**Email:** l.lombardo@utwente.it

## Abstract

Maps that attempt to predict landslide occurrences have essentially stayed the same since Brabb, E.E., Pampeyan, E.H. and Bonilla, M.G. (1972) Landslide susceptibility in San Mateo County, California (No. 360), US Geological Survey. The tools have certainly changed in fifty years. But, the geomorphological community addressed and still addresses this issue by estimating whether a given slope is potentially stable or unstable. This concept corresponds to the landslide susceptibility, a paradigm that entirely neglects how many landslides may trigger within a given slope, how large these landslides may be and what proportion of the given slope they may disrupt. Modeling how many landslides may occur per mapping unit has been recently proposed via the landslide intensity concept, which has later been shown to closely correlate to the planimetric extent of landslides per mapping unit. In this work, we take this observation a step further as we use the relation between landslide intensity and planimetric extent to generate maps that predict the aggregated size of landslides per mapping unit, and the proportion they may affect. Our findings suggest that it may be time for the geoscientific community as a whole, to revise the use of susceptibility assessment in favour of more informative analytical schemes. Our chain of landslide intensity, hazard and density may in fact lead to substantially improve decision-making processes related to landslide risk.

## Significance Statement

The geographic prediction of landslide occurrence is undertaken by assessing whether a slope may be stable or unstable. In other words, current practices treat slopes where a single landslide occurred in the same way as slopes where many landslides occurred. At the slope scale, this procedure inevitably underestimates the effect of multiple landslides. Here we model the number

2

of landslides per slope instead. Then, thanks to the close relation that the number of failures shows with respect to landslide size, we convert the estimated number of landslides into estimated landslide areas. Ultimately, we also estimate the expected proportion of a slope affected by landslides. This framework is more informative than the stable/unstable paradigm and may help landslide risk mitigation strategies.


**Introduction**

The international guidelines on managing the landslide threat in mountainous areas (1) have long stressed the need to report comprehensive information of landslide hazard. Specifically, in addition to the expectation of landslide occurrences across a given geographic space (and time), the size of the landslides are reported to be equally important (see also, 2). This information is commonly included in physically-based models (3) although the requirement of geotechnical data often limits the scope of the analyses at the catchment scale (4).

In a complementary manner, statistical models have the ability to cover large geographic areas, ranging from catchment to regional scales (5, 6). Such feat can be achieved because statistical models do not strictly require geotechnical parameters to be built. Instead, statistical models traditionally feature proxies of such mechanical properties, which nowadays can be obtained through remote sensing techniques (7). However, the current literature almost unanimously presents spatial models that evaluate whether a given mapping unit is expected to be stable or unstable (8). Therefore, these models inevitably neglect the potential number of landslides within a given mapping unit, as well as the expected planimetric area or volume associated with landslides triggered within the same unit.

An indication of the landslide size is separately computed and it refers to the landslide event magnitude (mL; 9). But, mL corresponds to a lumped measure which depends on the total number of mapped landslides and their overall planimetric extent. As a result, m}L is not spatially distributed but it is rather a single value associated to specific landslide events (10).

To extend the stable/unstable framework, the concept of landslide intensity was recently proposed (11). In this case, landslides are not treated in a binary way but as counts per mapping unit. The intensity was also shown to closely correlate to the cumulated landslide extent per mapping unit (see Figure 13 in 12). The latter contribution inspired the work we present here, by further exploiting the relation between intensity and landslide extent. Specifically, we propose a protocol to estimate the intensity first and later convert it to spatially predicted metrics linked to landslide size statistics per mapping unit.


**Materials and Methods**

This section will briefly introduce the study area and the landslide inventory we used. Subsequently, we will describe the spatial partition and the covariate set, together with the model we selected, referring to the articles where an extensive mathematical formulation is provided.

**Study area and landslide inventory**

The study area where we tested our modeling strategy is located within the Cinque Terre National Park, Italy. This park has become a UNESCO World Heritage Site in 1997 and has unfortunately experienced episodes of widespread landsliding in recent years (more details in 13). Figure 1 shows an overview of the study area and of the landslides triggered by the convective storm

occurred on October 25th 2011. During that day, up to 382 mm of rain were discharged in few hours, as recorded at the weather station of Monterosso (14).
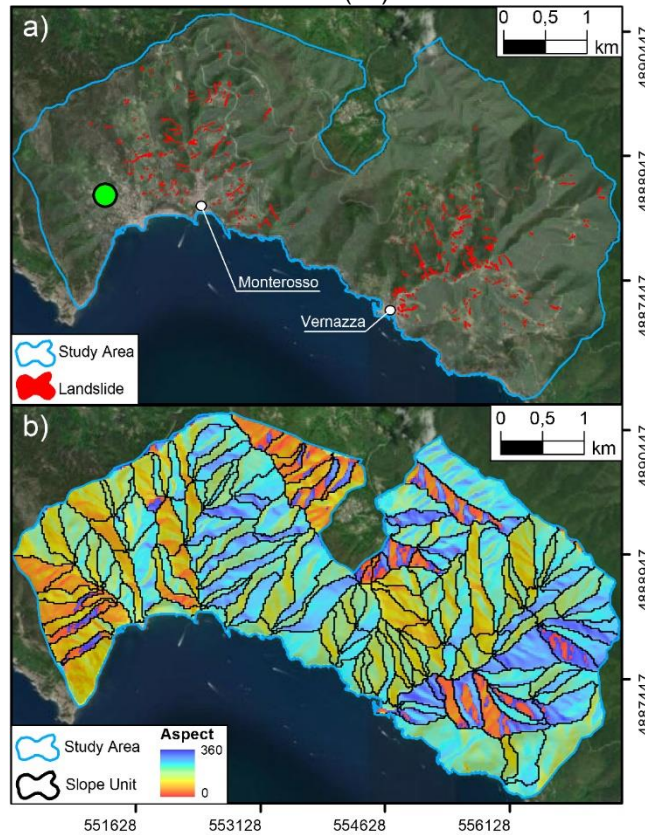


*Fig. 1. a) Overview of the landslide inventory and boundary of the study area; b) Slope Unit partition superimposed to the slope exposition. The green point corresponds to the location of the Monterosso weather station.*

**Mapping Units**
To model landslide intensity we chose a hierarchical structure. The high resolution mapping unit corresponds to grid-cells (GCs, 8). These are hierarchically combined with the coarser Slope Units (SUs, 15), at which level we computed the Latent Spatial Effect and we aggregated the intensity estimates (see 16). Specifically, we selected a 20~m resolution grid cell partition whereas we computed the SUs by using the *r.slopeunits* software (17). We parameterized *r.slopeunits* with a circular variance of 0.4, a minimum SU area of 12500 m$^2$ and a flow accumulation threshold of 100000 m$^2$. This operation returned 171 SUs.

**Covariate set**
The morphometric covariates we chose to build our intensity model were derived from a 5 m digital elevation model (DEM) accessed from the geo-portal of the Ligurian region (https://geoportal.regione.liguria.it/archivio-focus/item/662-dtm-\%E2\%80\%93-modello-digitale-del-terreno-\%E2\%80\%93-ed-2017.html). This DEM has been later resampled at 20 m resolution to match the squared lattice we defined. We computed the Euclidean distance from each GC to the nearest road or trail.
We also used the thematic properties described in (18). As a result, our covariate set featured: *i*) Elevation; *ii*) Slope Steepness; *iii*) Eastness; *iv*) Northness; *v*) Planar and *vi*) Profile Curvatures; *vii*)

Relative Slope Position; *viii*) Topographic Wetness Index; *ix*) Distance to road or trail; *x*) Land Use; *xi*) Terraced slope status; *xii*) Geology.

**Landslide Intensity Modeling**
The event inventory featured 695 landslides. By counting their distribution per mapping unit, we can model the resulting data as a Point Process. More specifically, we can define a Poisson Point Process as:

$$N(A) \sim Poisson \int_A \lambda(s)\,ds \qquad [1]$$

where *N(A)* is the number of expected landslides within the study area *A*, the selected sector of the Cinque Terre National Park in this case, *λ* is the intensity assumed to be ≥ 0, and *s* is each of the GC within the target area. This framework can be extended in its spatial form, conveniently expressing the intensity in logarithmic scale. This procedure gives rise to a Log-Gaussian Cox Process (LGCP), and in our case we expressed it as follows:

$$
\begin{aligned}
\log\{\lambda(s)\} &\sim Gaussian\ Process \\
&= \beta_0 + \sum_{J=1}^{J} \beta_j x_j(s) + f_{Geology} + f_{Land\ Use} + f_{Terraces} + f_{LSE}
\end{aligned} \qquad [2]
$$

where $\beta_0$ is the global intercept, $\beta_j$ are the fixed effects used to model continuous covariates and $f_{Geology}$, $f_{Land\ Use}$ and $f_{Terraces}$ are the random effects for categorical properties, whereas $f_{LSE}$ is the random effect for the  Latent Spatial Effect (LSE). The relation above corresponds to a Generalized Additive Mixed Models (GAMM, 19), which we implement here in its Bayesian form via INLA (20). We recall now two important properties of the landslide intensity. The intensity can always be converted into the most common susceptibility being the latter binary case a simpler realization of the count framework (21). This can be achieved as follows:

$$Susceptibility = 1 - e^{-\lambda_A} \qquad [3]$$

Also, handling the intensity information over space is more convenient than doing the same in the susceptibility case. In fact, the susceptibility is mapping-unit dependent whereas the intensity benefits from the Poisson aggregation property across any spatial units. In this work, we use this property to aggregate λ values estimated for each GC contained in a given SU (see Figure 5 in 16).

**From landslide intensity to hazard and density**
The landslide intensity has been shown to correlate with the total planimetric extent of landslides for each mapping unit (12). This contribution states that a model able to estimate landslide counts indirectly satisfies the current definition of hazard. However, the authors missed an important implication. In fact, if intensity and landslide sizes can be expressed one as the function of the other, this also means that one can convert landslide intensity maps into expected landslide size-related maps. In this work, we explore this possibility by estimating the intensity per SU and then estimating the landslide extent for each SU by multiplying the intensity for the mean landslide area. We then also take a step further by dividing the estimated landslide areas for the corresponding SU size, thus returning the landslide density.

**Performance assessment and model validation**
Being our GAMM hierarchical in nature, we separately evaluate the performance at the level of the two mapping units. At the GC scale, where the data is almost binary in nature, we use Receiver Operating Characteristic curves (22) and their integral or AUC (23). At the SU level, we check the agreement between observed landslide counts and aggregated intensities via $\chi^2$ test and the Spearman correlation coefficient (σ). We repeat the same performance evaluation also in a cross-

validation scheme. In this case, we opt for a Leave-one-out (L1O-CV) spatial cross validation where each of the 171 individual SUs is selected once at a time as a testing subset. A similar operation in the context of landslide modeling is extensively described in (24). In our case, we extract all the GCs contained in each SU. Thus, being the SU different in size, a different number of GCs is extracted for each spatial cross-validation run.

## Results

The goodness-of-fit and prediction-skill results are respectively shown in Figure 2, where the whole modeling procedure appears to suitably perform, irrespective of the considered mapping unit. Specifically, the AUC for the fit is equal to 0.92 (Fig. 2a), while the AUC obtained from the L1O is 0.91 (Fig. 2d). As for the count framework, the σ and the $\chi^2$ values confirm the close match between observed and modeled data both for the fit (Fig. 2b) and the L1O-CV (Fig. 2e). The same level of agreement is also confirmed through QQ-plots, with very few cases diverging from the bisector.
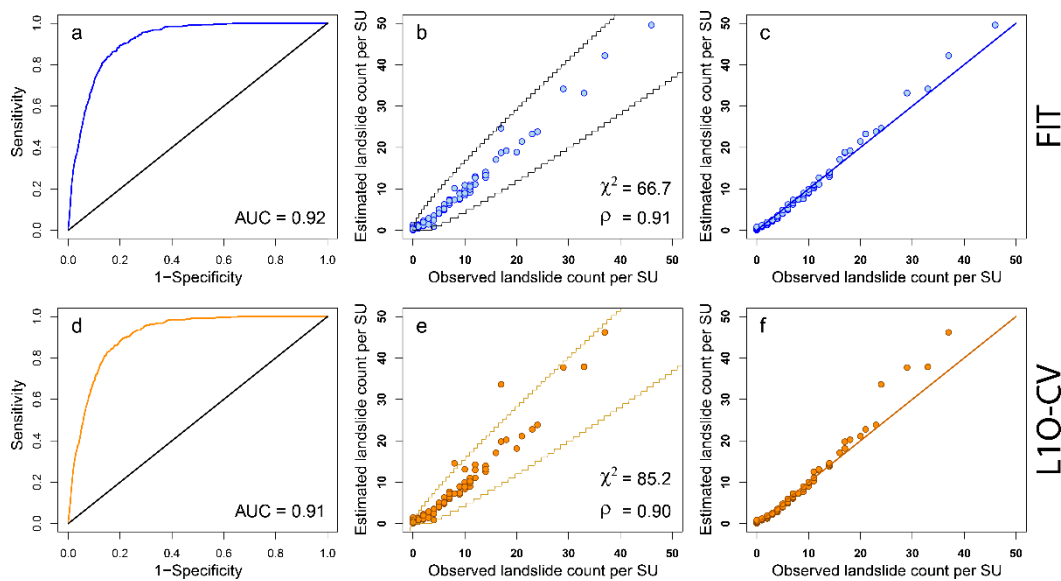


*Fig. 2. Performance assessment overview: the first row shows the goodness-of-fit whereas the second row reports the L1O-CV results. In the first column, we show the ROC curves and associated AUCs; the second column summarizes the match between observed and mod modeled counts, together with their χ2 tests; the third column illustrates the QQ-plots again between observed and modeled counts.*

Having demonstrated that the model performance are suitable to estimate the landslide intensity associated with the October 2011 event, we also provide an interpretation of the model components in the supplementary material.
As introduced in Section 1, Fig.13 in (12) showed that the intensity is closely related to landslide areas per SU. Therefore, we recreated the same plot to test whether this observation holds even in our study area. This is shown in Figure 3, where the above-mentioned relation appears to be

valid also for the shallow landslides mapped within the studied sector of the Cinque Terre National Park. Also, this relation does not get lost in the fitting and predicting phases.
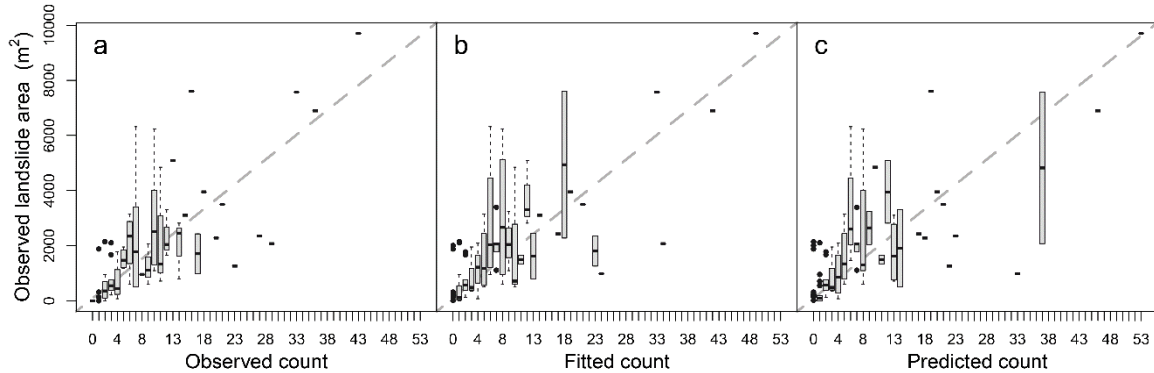


*Fig. 3. Association between landslide counts and areas aggregated at the SU level, for the observation (a), the fit (b) and the L1O-CV (c).*

We used the estimated landslide intensities to determine the expected landslide area aggregated per SU. This can be achieved by taking the product of the intensity times the mean landslide area per SU. However, the empirical mean of the landslide area distribution may be site specific, therefore, we tested whether we could generalize this information by estimating the theoretical mean. This operation follows the assumptions stated in (9), although here we extend the same idea to the spatial context.

Specifically, we fitted a series of statistical distributions (Gumbel, inverse-Gamma, double Pareto, log-Gaussian) to get an estimate of the population mean accounting for the heavy tail of the landslide area distribution. We found that both the Gumbel and double Pareto distribution provide a consistent estimate of the mean. We use this estimate to construct a plug-in estimator of the density of the landslide sizes distribution by multiplying it with the estimated intensity. The resulting landslide area distributions are shown in Figure 4, where the conversion from the Gumbel (or DP) appears to closely match the actual observational data. This result is the foundation of the first mapping procedure in the geoscientific literature where landslide areas as well as landslide densities are estimated in map form through data-driven model.
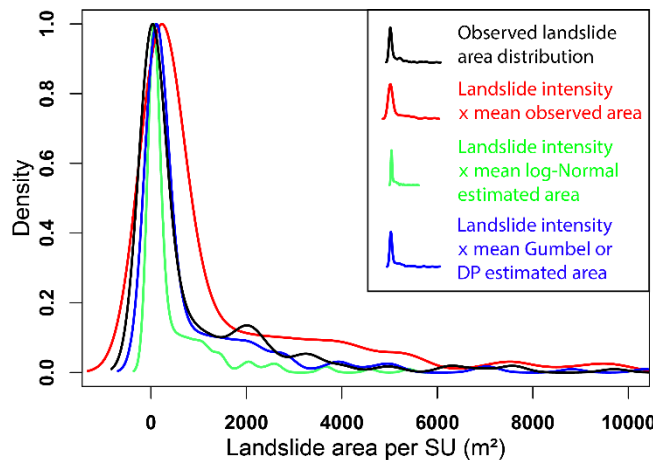


*Fig. 4. Landslide area distributions generated by multiplying the L1O-CV intensity to the empirical mean and the populations means obtained by through a Gumbel, inverse-Gamma, double Pareto (DP), log-Gaussian fits. The inverse-Gamma is not reported because the estimated mean tends to infinity. Also, the means estimated via the Gumbel and DP fits are equivalent.*

Figure 5 graphically summarized the aforementioned maps. The left column, making use of the fitted intensities, shows a pattern that closely matches the landslide distribution in Fig. 1. But, much more information is provided, with the expected number of landslides both at the GC and SU levels, together with the converted landslide area and density. The second column reports the deviation from the fit of the equivalent information. This is computed as the difference of the fitted results being subtracted from the L1O-predicted ones. The figure graphically stresses something already mentioned above, this being the stability of our landslide intensity framework. In fact, very narrow residuals are generally returned across the whole study area. And, the largest ones correspond to single slope units, where likely very localized landscape characteristics affect the distribution of the original landslide counts.
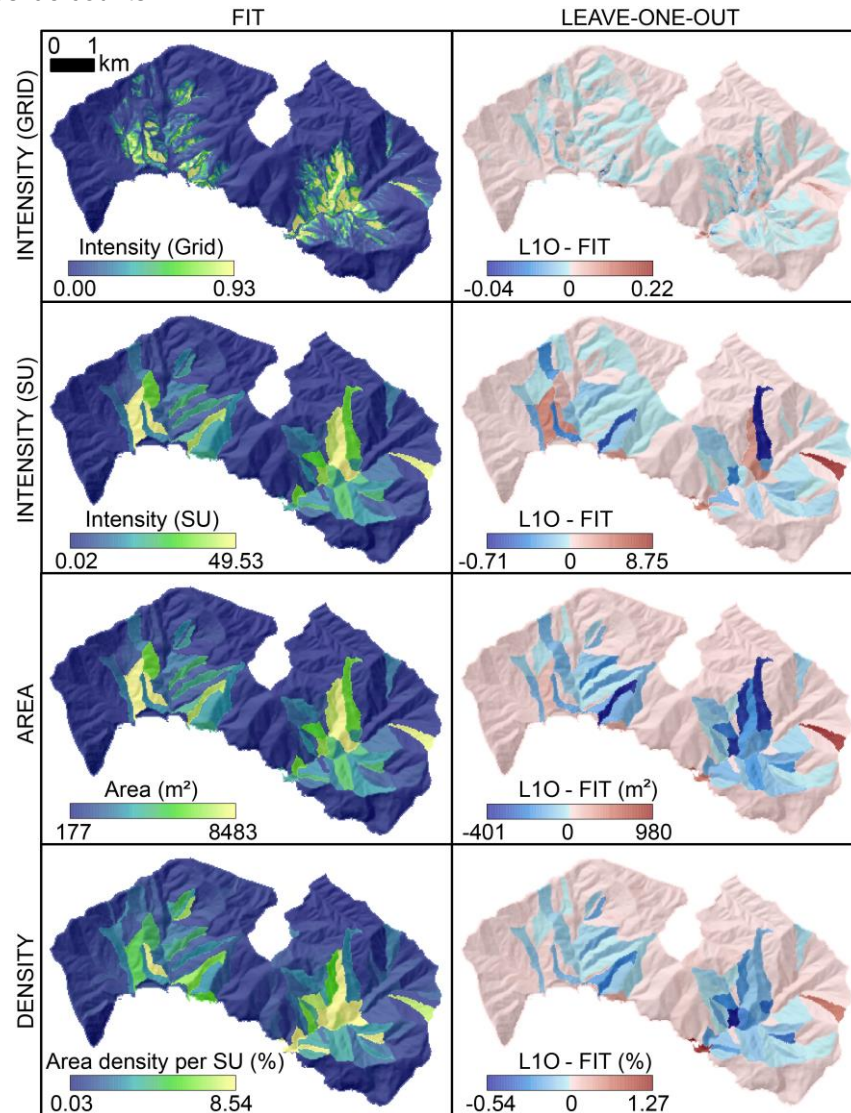


*Fig. 5. Intensity, hazard and density maps obtained by multiplying the Gumbel landslide area population mean to the fitted (first column) and L1O-predicted intensity.*

## Discussion

The workflow we propose has some unique features meant to address the landslide hazard definition (25). The omnipresent binary classification is left behind in favor of a count-oriented

model, which is further exploited to derive the expected landslide area and density per SU. The strength of this procedure resides in the advantages it brings with respect to the landslide susceptibility counterpart. In fact, whenever we apply a dichotomous classification to a given study site, we neglect the number of landslides that certain regions may exhibit. Therefore, we may heavily underestimate the threat that any urban settlement may be exposed to. If a SU contains tens of debris flows and another SU contains just one, a binary classifier will treat the two mapping units in the very same way. Conversely, the landslide intensity framework proposed by (11) respect the spatial information carried by the number of landslides per mapping unit. However, even the intensity framework has some weaknesses. For instance, the number of events may be difficult to interpret in terms of hazard because of amalgamation issues (26). Conversely, as also clearly stated in the most accepted definition of landslide hazard (25) and in the international guidelines (1), a much more informative parameter is the landslide area (27). It is also worth mentioning that a even better parameter is the landslide velocity or kinematic energy (28). However, this parameter can only be obtained via physically-based models and currently no large database exist to support data-driven models. Therefore, the landslide area is the most viable solution to estimate landslide hazard in the context of spatially-explicit models (alternatively one could use volumes, with all the uncertainties they introduce though (29)). The only example on this topic corresponds to (10). There, the authors modeled the aggregated landslide area per SU via a log-Gaussian GAM. However, even this case has its own weaknesses. The use of a log-Gaussian likelihood implies that the landslide area is expressed at the logarithmic scale, thus making the interpretation difficult. Moreover, a Log-Gaussian model works well for the bulk of a distribution but not for the tails. Thus, when transforming back from the logarithmic to the actual metric scale, the very small and very large landslides exhibit the largest errors. And, the large ones are also the most threatening ones, thus an error in the tail would result in a large underestimation of the landslide hazard. In addition to this issue, the model introduced by (10) uniquely targets the landslide area without accounting for the proneness to fail of a given slope. In other words, if the model estimates that a slope has the right characteristics to potentially release a large landslide, but the susceptibility is very low, then the hazard would also be very low. Therefore, our contribution fits in the context previously described by combining all the required information. The intensity intrinsically returns an estimate of which slopes are unstable, and through the actual number of expected landslides, we derive the expected landslide size and density per mapping unit.

**Concluding remarks**

Our model satisfies most of the requirements of the landslide hazard definition. However, because we used an event-based landslide inventory (30), our model lacks the temporal characteristic typical of the hazard context. To extend our model from the purely spatial to the spatio-temporal framework, the inventory must reflect multi-temporal occurrences. As a result, we could implement a space-time LGCP model whose intensities can be converted into expected landslide areas and density per mapping unit according to the user preferences. Also, our model relies on the assumption that as the number of landslides increases, the landslide area per mapping unit should also proportionally increase. This assumption may be valid but it may also be very site-dependent. In fact, certain slopes may give rise to single and large landslides whose planimetric area maybe much larger than many small landslides combined. In such situations, our assumption may not hold and therefore our model may not be applicable. In many sites, the underestimation brought by very large landslides may affect few if not single slopes. Thus, our approach could still be extremely valuable to assess the hazard across the whole study area. However, in structurally controlled landscapes where landslides tend to be generally large (e.g., 31), our approach may not be applicable. Also, this assumption has been mainly tested so far for translational landslides and debris flows. More tests are required to validate this assumption in various geographic contexts and different type of failure mechanisms.
Ultimately, the real advantage of the approach we propose has to do with available landslide inventories. The current tendency is for scientists to map landslides as polygonal features. This is clearly the most appropriate approach to mapping. However, the community has not standardized

this procedure and a large number of point-based inventories are continuously released, even through semi-automated mapping protocols (32, 33). But, even if starting from tomorrow, all landslides would be perfectly mapped and shared via polygonal inventories, this does not change the fact that five decades of geomorphological mapping has produces enormous point-based information. To estimate landslide intensity, one only needs number of landslides per mapping unit, an information easily estimated even with point data. This would by-pass the strict need for planimetric information and allow one to estimate the expected landslide area per mapping unit by converting the intensity. The only requirement would be to have access to a mean landslide area, likely connected to the landslide type and general tectonic and climatic setting, something largely demonstrated in a number of papers (9, 34, 35). As a result, one could mine a large amount of unused information and potentially convert five decades of traditional susceptibility maps into hazard ones.

## Acknowledgments

## References

1. R Fell, et al., Guidelines for landslide susceptibility, hazard and risk zoning for land-use planning. Eng. geology 102, 99–111 (2008).
2. DG Bellugi, DG Milledge, KM Cuffey, WE Dietrich, LG Larsen, Controls on the size distributions of shallow landslides. Proc. Natl. Acad. Sci. 118 (2021).
3. B van den Bout, et al., Towards a model for structured mass movements: the OpenLISEM hazard model 2.0a. Geosci. Model. Dev. 14, 1841–1864 (2021).
4. B Van den Bout, L Lombardo, M Chiyang, C van Westen, V Jetten, Physically-based catchment-scale prediction of slope failure volume and geometry. Eng. Geol. 284, 105942 (2021).
5. F Catani, D Lagomarsino, S Segoni, V Tofani, Landslide susceptibility estimation by random forests technique: sensitivity and scaling issues. Nat. Hazards Earth Syst. Sci. 13, 2815– 312 2831 (2013).
6. J Goetz, A Brenning, H Petschko, P Leopold, Evaluating machine learning and statistical prediction techniques for landslide susceptibility modeling. Comput. & geosciences 81, 1–11 (2015).
7. CJ Van Westen, E Castellanos, SL Kuriakose, Spatial data for landslide susceptibility, hazard, and vulnerability assessment: An overview. Eng. geology 102, 112–131 (2008).
8. P Reichenbach, M Rossi, BD Malamud, M Mihir, F Guzzetti, A review of statistically-based landslide susceptibility models. Earth-Science Rev. 180, 60–91 (2018).
9. BD Malamud, DL Turcotte, F Guzzetti, P Reichenbach, Landslide inventories and their statistical properties. Earth Surf. Process. Landforms 29, 687–711 (2004).
10. L Lombardo, H Tanyas, R Huser, F Guzzetti, D Castro-Camilo, Landslide size matters: A new data-driven, spatial prototype. Eng. Geol. 293, 106288 (2021).
11. L Lombardo, T Opitz, R Huser, Point process-based modeling of multiple debris flow landslides using INLA: an application to the 2009 Messina disaster. Stoch. environmental research risk assessment 32, 2179–2198 (2018).
12. L Lombardo, T Opitz, F Ardizzone, F Guzzetti, R Huser, Space-time landslide predictive modelling. Earth-Science Rev. 209, 103318 (2020).
13. M Di Napoli, et al., Machine learning ensemble modelling as a tool to improve landslide susceptibility mapping reliability. Landslides 17, 1897–1914 (2020).
14. A Cevasco, et al., Storminess and geo-hydrological events affecting small coastal basins in a terraced Mediterranean environment. Sci. Total. Environ. 532, 208–219 (2015).

15. A Carrara, M Cardinali, F Guzzetti, P Reichenbach, GIS technology in mapping landslide hazard in Geographical information systems in assessing natural hazards. (Springer), pp. 335–175 (1995).
16. L Lombardo, et al., Geostatistical modeling to capture seismic-shaking patterns from earthquake-induced landslides. J. Geophys. Res. Earth Surf. 124, 1958–1980 (2019).
17. M Alvioli, et al., Automatic delineation of geomorphological slope units with r. slopeunits v1.0 and their optimization for landslide susceptibility modeling. Geosci. Model. Dev. 9, 3975– 3991 (2016).
18. M. Di Napoli, et al., Rainfall-Induced Shallow Landslide Detachment, Transit and Runout Susceptibility Mapping by Integrating Machine Learning Techniques and GIS-Based Approaches. Water 13, 488 (2021).
19. S Steger, et al., Correlation does not imply geomorphic causation in data-driven landslide susceptibility modelling–Benefits of exploring landslide data collection effects. Sci. total environment 776, 145935 (2021).
20. H Bakka, et al., Spatial modeling with R-INLA: A review. Wiley Interdiscip. Rev. Comput. Stat. 10, e1443 (2018).
21. L Lombardo, T Opitz, R Huser, Numerical recipes for landslide spatial prediction using R-INLA: a step-by-step tutorial in Spatial modeling in GIS and R for earth and environmental sciences. (Elsevier), pp. 55–83 (2019).
22. DW Hosmer Jr, S Lemeshow, RX Sturdivant, Applied logistic regression. (John Wiley & Sons) Vol. 398, (2013).
23. O Rahmati, et al., PMT: New analytical framework for automated evaluation of geoenvironmental modelling approaches. Sci. total environment 664, 296–311 (2019).
24. S Steger, A Brenning, R Bell, T Glade, The propagation of inventory-based positional errors into statistical landslide susceptibility models. Nat. Hazards Earth Syst. Sci. 16, 2729–2745 (2016).
25. F Guzzetti, A Carrara, M Cardinali, P Reichenbach, Landslide hazard evaluation: a review of current techniques and their application in a multi-scale study, Central Italy. Geomorphology 31, 181–216 (1999).
26. H Tanyaş, CJ van Westen, KE Allstadt, RW Jibson, Factors controlling landslide frequency–area distributions. Earth surface processes landforms 44, 900–917 (2019).
27. DL Turcotte, BD Malamud, F Guzzetti, P Reichenbach, Self-organization, the cascade model, and natural hazards. Proc. Natl. Acad. Sci. 99, 2530–2537 (2002).
28. J Corominas, et al., Recommendations for the quantitative analysis of landslide risk. Bull. engineering geology environment 73, 209–263 (2014).
29. IJ Larsen, DR Montgomery, O Korup, Landslide erosion controlled by hillslope material. Nat.Geosci. 3, 247–251 (2010).
30. F Guzzetti, et al., Landslide inventory maps: New tools for an old problem. Earth-Science Rev. 112, 42–66 (2012).
31. H Tanyaş, K Hill, L Mahoney, I Fadel, L Lombardo, The world's second-largest, recorded landslide event: Lessons learnt from the landslides triggered during and after the 2018 Mw 7.5 Papua New Guinea earthquake. Eng. Geol. 297, 106504 (2022).
32. G Amato, C Eisank, D Castro-Camilo, L Lombardo, Accounting for covariate distributions in slope-unit-based landslide susceptibility models. a case study in the alpine environment. Eng. geology 260, 105237 (2019).
33. P Amatya, D Kirschbaum, T Stanley, Rainfall-induced landslide inventories for Lower Mekong based on Planet imagery and a semi-automatic mapping method. Geosci. Data J. n/a (year?).
34. FE Taylor, BD Malamud, A Witt, F Guzzetti, Landslide shape, ellipticity and length-to-width ratios. Earth Surf. Process. Landforms 43, 3164–3189 (2018).
35. G Amato, L Palombi, V Raimondi, Data–driven classification of landslide types at a national scale by using Artificial Neural Networks. Int. J. Appl. Earth Obs. Geoinformation 104, 102549384 (2021).

# Supplementary Materials

**Description of the linear/fixed effects**

Here, we report a summary of the fixed effects estimated to be significant. Hence, with a 95% Credible Interval that does not cross the zero line of the regression coefficient. In other words, we consider significant a covariate whose 2.5 and 97.5 percentiles share the same sign. Whether this is negative or positive, it will only influence the interpretation. However, in this work, four significant covariates were estimated by our LGCP (Log-Gaussian Cox Process) namely, Elevation, Planar Curvature, Relative Slope Position and Distance to road or trail. They are shown in Figure S1, where they stand out to reduce the estimated landslide intensity. The role of the elevation could be interpreted as a result of the dissipation of the auto-regenerative cloudburst coming from the sea. In fact, the storm responsible for the landslides we mapped came from theTyrrhenian Sea (south of the study area) and quickly released the rainfall as it moved uphill. Thus, the vast majority of landslides clusters at medium elevations. This effect is relatively common in similar steep coastal settings and an exact analogous example can be found in Lombardo et al. (2015). The role of the Planar Curvature can be interpreted in terms of favorable morphologies to slope instability. Specifically, a negative regression coefficient implies that laterally convex shapes contribute to decrease the expected number of landslides. Conversely, laterally concave morphologies contribute to increase the landslide intensity. The negative role of the Relative Slope Position reaffirms that landslides predominantly triggered half-way through the topographic profile (e.g., Desmore and Hovius, 2000). As for the distance to road or trail, a negative mean regression coefficient could be interpreted with an anthropic control on the slope stability. In fact, a negative sign implies that the intensity decreases as the distance increases. Thus, locations proximal to road cuts or trails are estimated to contribute to the intensity estimation (e.g., Tanyas et al., 2022). These lineaments not only may destabilize a slope modifying the previous equilibrium. But, they also modify the hydrological behavior of overland flows, establishing surfaces with reduced permeability and subsequently increasing the runoff, which in turn can bring instability in the lower sections of the topographic profile.
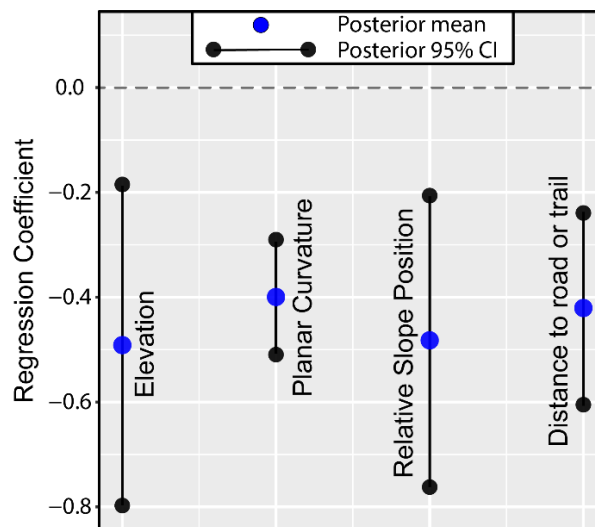


**Figure S1.** Posterior means (blue dots) of significant fixed effects, together with their 95% credible intervals (black dots). The horizontal black dashed lines indicate no contribution to the landslide intensity.

**Description of the nonlinear/random effects**

Here, we report a summary of the random effects by plotting their posterior means together with their 95% credible intervals (see Figure S2). The panel reports covariates that have been used in a purely categorical form, i.e., with class effects being mutually independent a priori (this is the case for Land Use, Terraced slopes Status and Geology). As for covariates that have been modeled with some degree of dependence, we have two examples. The first one corresponds to the Slope Steepness. This covariate has been binned into twenty classes, with a constraint of adjacent class dependence driven by a random walk of the first order (RW1, see Ruiz-Cárdenas et al., 2010). The second case corresponds to a Latent Spatial Effect (LSE, see Bakka et al., 2018). In this work we have opted for a Besag model (Martino and Rue, 2009). This model essentially corresponds to a RW1 in two dimensions and contributes to drive dependence across the geographic space. Specifically, the adjacent matrix computed for the slope unit partition provides the structure upon which the Besag is run, and makes it so that close slope units behave more similarly than slope units far away from each other. In Figure S2, the first covariate we present is the Slope Steepness. Its nonlinear effect appears to be quite sigmoidal, with three main sections. The range between 0° and 25° contributes to decrease the expected landslide intensity, albeit within this range the negative contribution decreases down to negligible effects at 25°. Then, from this value up to roughly 40°, the contribution to the landslide intensity increases quite linearly, only to flatten from 40° to the maximum steepness of around 65°. This behavior is in line with the type of landslides we consider, i.e. superficial and rapid landslides (Cevasco et al., 2013).
Concerning Land Use, LU7 and LU8, namely vineyards and abandoned vineyards respectively, contribute to increase the landslide intensity. This is also in agreement with the literature on shallow landslides in the Cinque Terre (Cevasco et al., 2014; Brandolini et al., 2018; Di Napoli et al., 2021). This also stands out in the Terraced slopes Status covariate. Cultivated terraces areas (T2) and, especially, abandoned terraces with poor vegetation cover (T3) appear prone to instability. Along these lines, Pepe et al. (2019) conducted a detailed investigation on land-use transformations from the early 1950s to 2011, analyzing the influence that the abandonment of cultivated terraced slopes exerted on the distribution and magnitude of rainfall-induced shallow landslides. Geology is not to be considered secondary in these analyses. Although most of the classes appear to be non-significant, G2 (or Canetolo Shales and Limestones) positively contributes to the landslide intensity. This politic-dominant and impermeable type of bedrock can be responsible for the genesis of widespread slope failures (Cevasco et al., 2014). Ultimately, the LSE shows that the easternmost sector of the study area is linked to the highest positive residuals between observed and estimated intensities. This pattern briefly transitions to negative values and assumes positive LSE values in the westernmost region of the study area. This may have to do to with the spatio-temporal pattern of the cloudburst and how the rainfall may have been discharged through the study area (Cevasco et al., 2015).
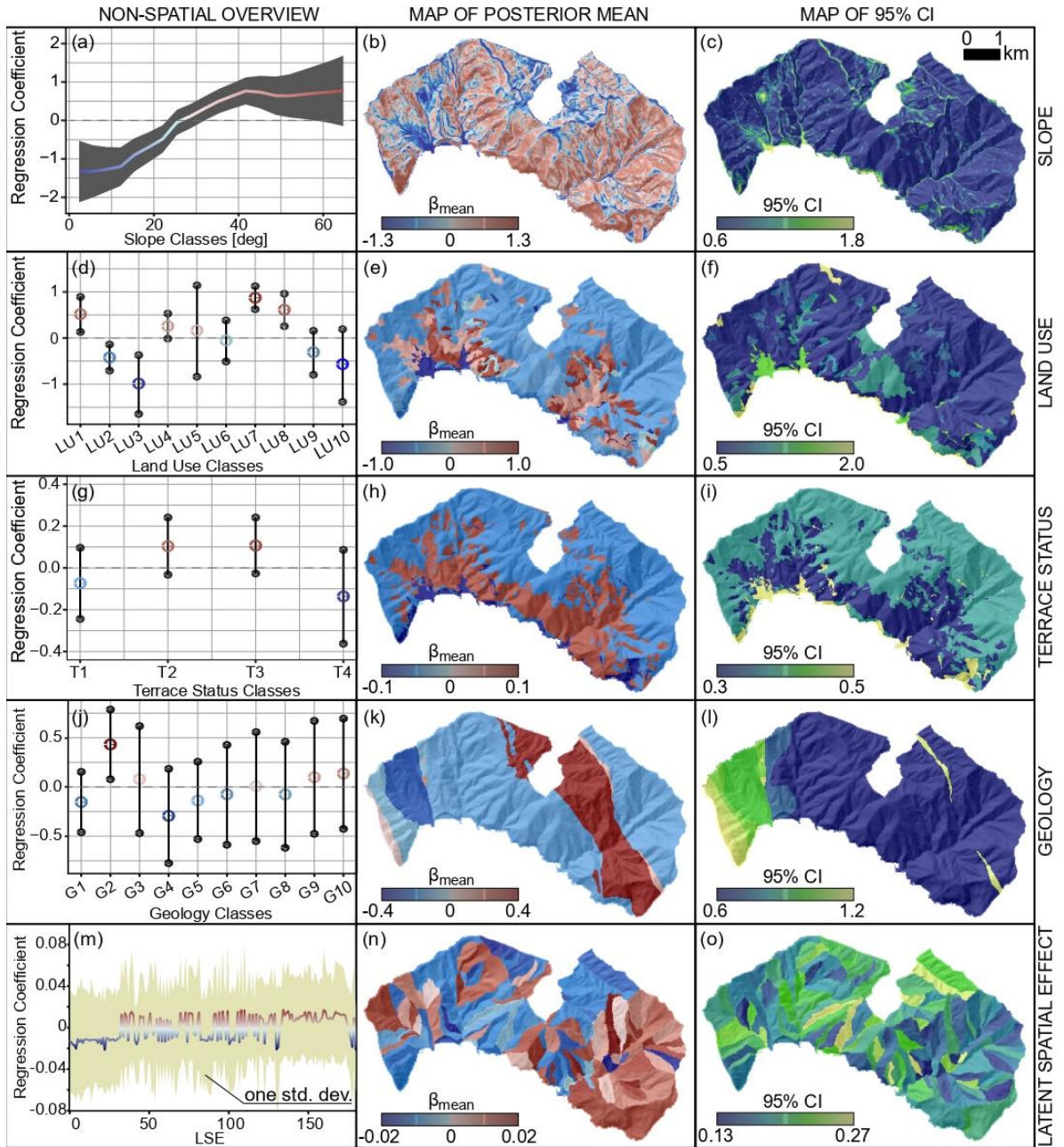
**Figure S2.** Random effects for the performed model, from top to bottom: slope ranging from 0 to 90 degrees, land use classes (LU1 = Complex Cultivation Patterns, LU2 = Mixed Forest, LU3 = Urban and Industrial Area, LU4 = Olive Groves, LU5 = Moors and Scrubs, LU6 = Abandoned Olive Groves, LU7 = Vineyards, LU8 = Abandoned Vineyards, LU9 = Sclerophyllous Vegetation, LU10 = Beaches, Dunes, Sands and Bare rocks), agricultural terraced slopes status (T1 = abandoned terraces with dense vegetation cover - advanced state of abandonment, T2 = cultivated terraced areas, T3 = abandoned terraces with poor vegetation cover - initial state of abandonment, T4 = non-terraced areas - including either urban areas, outcropping rocks and woods), geology (G1 = Macigno Sandstones, G2 = Canetolo Shales and Limestones, G3 = T. Pignone Marls, G4 = Gabbros, G5 = M.te Veri Argillites and Limestones, G6 = Serpentinites, G7 = Gottero Sandstones, G8 = Val Lavagna Schists, G9 = Basalts and G10 = Cherts) and Latent Spatial Effect.